

# Relativistic correction to the dissociation temperature of $B_c$ mesons in the hot medium

Guangyu Li,<sup>1</sup> Baoyi Chen,<sup>1</sup> and Yunpeng Liu<sup>1,\*</sup>

<sup>1</sup>*Department of Applied Physics, Tianjin University, Tianjin 300350, China*

By solving two body Dirac equations with potentials at finite temperature, we calculated the dissociation temperature  $T_d$  of  $B_c$  mesons in the quark-gluon plasma. It is found that the  $T_d$  becomes higher with the relativistic correction than the  $T_d$  from the Schrödinger equation. The differences between them are analyzed and discussed.

PACS numbers: 25.75.Nq, 12.38.Mh, 25.75.-q

## I. INTRODUCTION

The phase transition between the quark-gluon plasma(QGP) and the hadron phase is one of the most interesting topics in the relativistic heavy ion physics. As the QGP can not be detected directly, the heavy quarkonium consisting of a heavy quark and a heavy antiquark has been proposed as a probe for the early stage of the hot medium in heavy-ion collisions [1–11]. Non-relativistic approximation is usually taken in the studies of heavy quarkonium, due to its large mass [7, 12–15]. Such an approximation is usually reasonable at zero temperature when the mass or radius is calculated, because the typical energy scale of the potential is smaller than the masses of heavy quarks.

However, the dissociation with a screened potential is different. The temperature as a new low energy scale comes in. The potential pulls the quarks together into a meson, and the temperature weakens the attraction. Around the maximum survival temperature, that is the dissociation temperature  $T_d$ , the balance between the attractive potential and the screening can be destroyed even by a relatively small contribution in the potential. Therefore, it is interesting to check how much change in temperature can rebalance the relativistic correction. Determining the in-medium properties of quarkonium is crucial for extracting the heavy quark potential at finite temperatures and also the hot medium information with the quarkonium probes. Some theoretical studies [16–18] about the relativistic effect have been done in open and hidden heavy flavors based on two body Dirac equations (TBDE) [19–22].

An analog to heavy quarkonia is the  $B_c$  meson [23–27], since it is composed of two heavy quarks. It is even a cleaner probe than heavy quarkonia, because (i) it is composed of heavy quarks with different flavor, so that the possible processes are less than heavy quarkonia, and (ii)  $B_c$  is a pseudo-scalar meson, so that the spin structure is simpler. It is therefore urgent to study the properties of the  $B_c$  meson at finite temperatures. In experiments, the nuclear modification factor of  $B_c$  mesons has been measured, and more helpful results can be expected

in the future [28]. In this work, we will employ TBDE compared with the Schrödinger equation to study the relativistic correction on  $B_c$  dissociation temperature.

## II. TBDE FOR $B_c$ MESONS AT FINITE TEMPERATURE

The TBDE is a generalization of the free Dirac equation. It is both relativistic and Schrödinger-like, and it has been used to calculate the meson spectra in vacuum and at finite temperature. In general, it is complicated coupled equations [16, 22]. For a (pseudo-)scalar meson, it decouples from the spin triplet components, and its equation can greatly be simplified. We rewrite its radial equation as

$$\left[ -\frac{d^2}{dr^2} + \Phi_{SI} + \Phi_1 \right] U(r) = b^2 U(r),$$

with

$$\begin{aligned}\Phi_{SI} &= 2m_w S + 2\varepsilon_w A + S^2 - A^2, \\ \Phi_1 &= \frac{1}{R} \frac{d^2}{dr^2} R, \\ R &= r \sqrt{\frac{(m_1 \varepsilon_2 + m_2 \varepsilon_1) X}{\varepsilon_1 M_2 + \varepsilon_2 M_1 - A(M_1 + M_2)}}, \\ M_i &= \sqrt{m_i^2 + Y/X}, \quad (i = 1, 2) \\ Y &= 2m_w S + S^2, \\ X &= 1 - \frac{2A}{m_m}.\end{aligned}$$

Here  $r$  is the radius of the relative motion. The quantities denoted by capital letters are all  $r$ -dependent functions. This convention is also kept elsewhere in this paper except for conventional special functions, the temperature  $T$ , and  $r$  itself. The  $r$ -independent quantities are the constituent mass of each quark  $\varepsilon_i$ , the reduced mass  $m_w$ , the energy  $\varepsilon_w$  of the imaginary particle for relative motion, and the eigenvalue-like term  $b^2$ , which are defined as

$$\begin{aligned}\varepsilon_i &= \frac{m_m^2 + 2m_i^2 - m_1^2 - m_2^2}{2m_m}, \quad (i = 1, 2) \\ m_w &= \frac{m_1 m_2}{m_m},\end{aligned}$$

\*Electronic address: Email:yunpeng.liu@tju.edu.cn

$$\varepsilon_w = \frac{m_m^2 - m_1^2 - m_2^2}{2m_m},$$

$$b^2 = \frac{m_m^4 - 2(m_1^2 + m_2^2)m_m^2 + (m_1^2 - m_2^2)^2}{4m_m^2}.$$

The inputs of such an equation are the charm quark mass  $m_1$ , the bottom quark mass  $m_2$ , and the potential between them divided into a scalar part  $S$  and a vector part  $A$ , while the outputs are both the mass  $m_m$  of the  $B_c$  meson and its radial wave function  $U(r)$ , so that the probability to find the quark pairs in a sphere shell  $r \sim r + dr$  is proportional to  $|U^2(r)|dr$ . Note that  $m_m$  appears on both sides of the equation. Therefore, it is actually not a typical eigen equation.

In the non-relativistic limit  $A, S \ll m_1, m_2, m_w, m_m$ , one find  $X \rightarrow 1$ ,  $M_i \rightarrow m_i$ ,  $R \rightarrow r$ ,  $\Phi_1 \rightarrow 0$ ,  $\varepsilon_w \rightarrow m^S$ ,  $m_w \rightarrow m^S$  with the non-relativistic reduced mass  $m^S = \frac{m_1 m_2}{m_1 + m_2}$ , the spin-independent term  $\Phi_{SI} \rightarrow 2m^S V^S$  with  $V^S = A + S$  being the non-relativistic potential, and  $b^2 \rightarrow 2m^S \varepsilon$ , with  $\varepsilon = m_m - m_1 - m_2$  being the eigen energy in a Schrödinger equation. As expected, it reduces to a Schrödinger equation

$$\left[ -\frac{1}{2m^S} \frac{d^2}{dr^2} + V^S \right] U(r) = \varepsilon U(r),$$

or

$$\left[ -\frac{1}{2m^S} \frac{d^2}{dr^2} + \bar{V}^S \right] U(r) = -\Delta\varepsilon^S U(r),$$

with the non-relativistic binding energy  $\Delta\varepsilon^S = m_1 + m_2 + v_\infty - m_m$ . Here we have introduced the shifted potential  $\bar{V}^S = V^S - v_\infty$ ,  $v_\infty = \lim_{r \rightarrow +\infty} V^S$ , so that  $\bar{V}^S$  vanish at  $r \rightarrow +\infty$ . Such a bar-symbol is also used for other potentials in the following.

A widely used potential  $V^S$  in vacuum is the Cornell potential which contains a Coulomb-like potential  $A = -\frac{\alpha}{r}$ , and a linear potential  $S = \sigma r$ . Charmonium and Bottomonium spectra can be fitted with  $\alpha = \pi/12$  and  $\sigma = 0.2 \text{ GeV}^2$  [12]. At finite temperature, we take the screened Cornell potential [12] as a function of the screening mass  $\mu$  and radius  $r$ ,

$$V^S(r, \mu) = A(r, \mu) + S(r, \mu),$$

$$A(r, \mu) = -\alpha\mu \left( \frac{e^{-\mu r}}{\mu r} + 1 \right),$$

$$S(r, \mu) = \frac{\sigma}{\mu\Gamma(\frac{3}{4})} \left[ \frac{\Gamma(\frac{1}{4})}{2^{\frac{3}{2}}} - \frac{(\mu r)^{\frac{1}{2}}}{2^{\frac{3}{4}}} K_{\frac{1}{4}}(\mu^2 r^2) \right],$$

We have attributed the screened Coulomb-like potential to  $A$ , and the screened confining potential to  $S$ , as it is at zero temperature [29]. This is our assumption in the main part of this paper, and we will revisit it in the end. The only temperature dependent parameter is the screening mass  $\mu$ , which we fit from the lattice result [30] as

$$\mu(\bar{T})/\sqrt{\sigma} = s\bar{T} + \sqrt{\frac{\pi}{2}} a\sigma_t \left[ \text{erf}\left(\frac{b}{\sqrt{2}\sigma_t}\right) - \text{erf}\left(\frac{b - \bar{T}}{\sqrt{2}\sigma_t}\right) \right],$$

with  $\bar{T} = T/T_c$ ,  $\text{erf}(t) = \frac{2}{\sqrt{\pi}} \int_0^t e^{-x^2} dx$ ,  $s = 0.587$ ,  $a = 2.150$ ,  $b = 1.054$ , and  $\sigma_t = 0.07379$ .

The only free parameters left are quark masses  $m_1$  and  $m_2$ . We fit masses of scalar heavy mesons composed of a charm quark and/or a bottom quark in experiments [31] to obtain  $m_1$  and  $m_2$  both in TBDE and in the Schrödinger equation. The results are listed in Table I. We denote the results or parameters for the Schrödinger equation with a superscript  $S$ , and those for TBDE with a superscript  $D$  to distinguish them when necessary.

	$m_1$	$m_2$	$m_{\eta_c}$	$m_{\eta_b}$	$m_{B_c}$
Schrödinger Eq.	1.19	4.59	2.991	9.415	6.256
TBDE	1.27	4.62	2.997	9.421	6.254
Experiments	-	-	2.984	9.399	6.274

TABLE I: Mass parameters in the Schrödinger equation and those in TBDE. The units of masses in the table are all GeV. Experimental data are from the Particle Data Group [31].

### III. RESULTS AND DISCUSSIONS

At finite temperature, the binding energy  $\Delta\varepsilon$  of  $B_c$  is defined as the energy difference between the lowest scattering state and the bound state

$$\Delta\varepsilon^D = v_\infty + \sqrt{v_\infty^2 + (m_1 + m_2)^2} - m_m^D,$$

while in the non-relativistic limit, it becomes  $\Delta\varepsilon^S = v_\infty + m_1 + m_2 - m_m^S$  as mentioned above. The temperature dependence of the binding energy  $\Delta\varepsilon$ , and that of the average radius

$$\langle r \rangle = \frac{\int dr r |U(r)|^2}{\int dr |U(r)|^2},$$

and the  $r$  dependence of the wave functions  $U$  of  $B_c$  are shown in Fig. 1, Fig. 2, and Fig. 3, respectively. It can

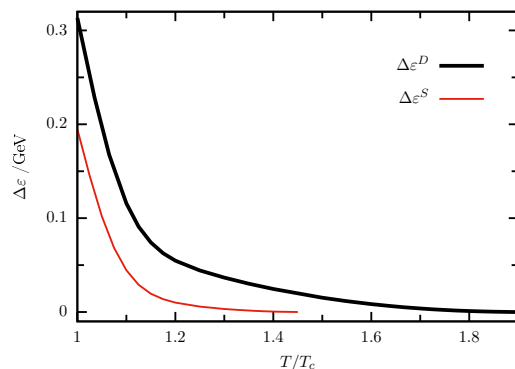


FIG. 1: Binding energy  $\Delta\varepsilon$  as a function of temperature  $T$  compared with the non-relativistic limit.

be seen that in both cases, the higher the temperature is,

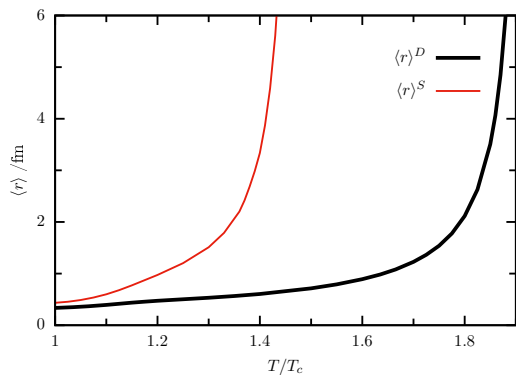


FIG. 2: Average radius as a function of temperature  $T$  compared with the non-relativistic limit.

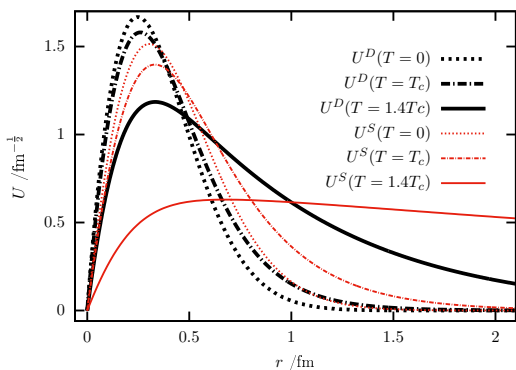


FIG. 3: Wave functions at different temperatures  $T = 0$ ,  $T = T_c$  and  $T = 1.4T_c$ .

the weaker the binding between the two heavy quarks is, as expected. The dissociation temperature  $T_d$ , at which the binding energy reduces to zero, increases from  $1.45T_c$  to  $1.9T_c$  when the relativistic correction is considered.

To understand the differences, we firstly check the parameters  $m_1$  and  $m_2$  dependence. It is found that this factor is less important. For example, if the TBDE parameters  $m_1$  and  $m_2$  (see the middle row in Table I) instead are used in the Schrödinger equation, the dissociation temperature  $T_d$  will increase only by about only  $0.05T_c$ . This indicates that the differences in  $T_d$  are mainly due to the relativistic corrections in the equations, instead of the parameter difference in Table 1.

Now we turn to the difference in equations. A direct comparison is to compare  $\Phi$ . However, a potential is more intuitive. Therefore, we consider potentials  $V$  with and without the relativistic corrections at different temperatures  $T_c$  and  $1.4T_c$ , with  $V^D \equiv \frac{1}{2m_s} (\Phi_{SI} + \Phi_1)$ . For a better comparison, we plot  $\bar{V}$  in practice in Fig. 4 instead of  $V$ . That is we have dropped the finite constant term at  $r \rightarrow +\infty$  in the potential. It can be seen that at  $r \rightarrow 0$ , the temperature dependence of  $\bar{V}$  is relatively weak because at short distance it is dominated by the Coulomb term and the screening of it is weak, while at

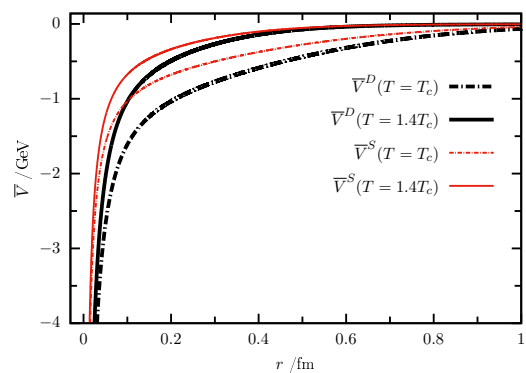


FIG. 4: Potentials as functions of radius  $r$  at temperatures  $T = T_c$  and  $T = 1.4T_c$ .

$r \rightarrow +\infty$ , we have  $\bar{V}^S \approx \bar{V}^D$ , which is reasonable since a large radius corresponds to a low energy scale, and the relativistic effect is less important. The potential well becomes deeper at lower temperature and/or in the relativistic case.

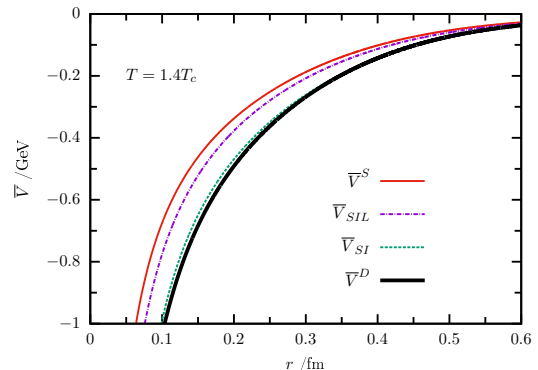


FIG. 5: Potentials as functions of radius  $r$  at temperature  $T = 1.4T_c$ .

The potential term is dominated by  $\Phi_{SI}$ , which means that the dissociation temperature of  $B_c$  meson is not sensitive to the spin structure. Actually, up-to the next-to-leading order of the non-relativistic approximation, we have

$$R = r \left[ 1 + \frac{\sec^2 \theta}{m_m} A - \frac{\sec^2 \theta + \tan^2 \theta}{m_m} S \right],$$

with  $\sin \theta = (m_1 - m_2)/m_m$ . The leading term of  $\Phi_1$  is

$$\begin{aligned} \Phi_1 &= \frac{1}{m_m r} [\sec^2 \theta (rA)'' - (\sec^2 \theta + \tan^2 \theta) (rS)'] \\ &\sim \frac{\mu^2}{m_m} \bar{V}^S. \end{aligned} \quad (1)$$

which implies that  $\Phi_1$  is roughly smaller than  $m_m V^S$  by a factor of  $\frac{\mu^2}{m_m^2}$ , and thus roughly smaller than  $\Phi_{SI} \approx 2m_w V^S$  by a factor of  $\frac{\mu^2}{2m_1 m_2}$ . At the temperature that

the  $B_c$  meson dissociates the screening mass is roughly 0.6 GeV, so that  $\Phi_1$  is only as small as few percents of  $\Phi_{SI}$ , and thus can be neglected, as shown in Fig. 5 with  $V_{SI} = \Phi_{SI}/(2m^S)$  and  $V^D = (\Phi_{SI} + \Phi_1)/(2m^S)$ . In this case, TBDE deduce to a relativistic two body equation for spinless particles [22].

The leading term in  $\Phi_{SI}$  is  $\Phi_{SIL} = 2m_w S + 2\varepsilon_w A$ , which differs from the non-relativistic potential in the mass terms. The masses at  $T = T_c$  and  $T = 1.4T_c$  are listed in Table II. It can be seen that the modification to the scalar part of the potential is relatively small (a few percents), while that to the vector part is relatively large (about 30%). As a result, the modification due the the mass coefficient is roughly at the order of 15%. (See the curve of  $\bar{V}_{SIL} = \Phi_{SIL}/(2m^S)$  in Fig. 5.)

$T/T_c$	$m_m$	$m^S$	$m_w$	$\varepsilon_w$
1.0	6.217	0.945	0.944	1.262
1.4	6.111	0.945	0.960	1.177

TABLE II: Masses in  $\Phi_{SIL}$ . All the units of masses in the table are GeV.

Note that there is some ambiguity from the non relativistic potential  $V^S$  to the potential  $\Phi_{SI} + \Phi_1$  in TBDE, because it depends on how it is divided into the vector part  $A$  and the scalar part  $S$ , especially when the potential is given numerically as in the lattice QCD. We tried

to attribute both the  $v_\infty$  terms to the scalar potential, leaving  $A = -\alpha e^{-\mu r}/r$ . Then the dissociation temperature shifts from  $1.9T_c$  to  $1.7T_c$ . Actually, we can rewrite  $\Phi_{SI}$  under the approximation  $m_w \approx m^S$  and  $\varepsilon_w \approx m^S$  as  $\Phi_{SI} \approx 2m^S V^S (1 + (S - A)/(2m^S))$ . Therefore, the larger  $S - A$  is, the deeper the well is. In the trial scheme in this paragraph,  $S - A$  became smaller, and the binding is looser.

#### IV. SUMMARY

In summary, the dissociation temperature of  $B_c$  meson in QGP is calculated by TBDE, and it is found to be higher than that by Schrödinger equation. The spin dependent part is negligible, and the increase is mainly due to the square term in the spin independent part of the potential  $\Phi_{SI}$ .

#### Acknowledgement

This work is supported by the National Natural Science Foundation of China (NSFC) under Grant No. 12175165. Liu is grateful to Prof. Xingyu Guo for helpful discussions.

- 
- [1] T. Matsui and H. Satz.  $J/\psi$  Suppression by Quark-Gluon Plasma Formation. *Phys. Lett. B*, 178:416–422, 1986.
- [2] Xiao-Ming Xu, D. Kharzeev, H. Satz, and Xin-Nian Wang.  $J/\psi$  suppression in an equilibrating parton plasma. *Phys. Rev. C*, 53:3051–3056, 1996.
- [3] Robert L. Thews, Martin Schroedter, and Johann Rafelski. Enhanced  $J/\psi$  production in deconfined quark matter. *Phys. Rev. C*, 63:054905, 2001.
- [4] Peng-fei Zhuang and Xiang Lei Zhu. Leakage effect on  $J/\psi$   $p_t$  distributions in different centrality bins for Pb Pb collisions at  $E/A=160$  GeV. *Phys. Rev. C*, 67:067901, 2003.
- [5] Li Yan, Pengfei Zhuang, and Nu Xu. Competition between  $J/\psi$  suppression and regeneration in quark-gluon plasma. *Phys. Rev. Lett.*, 97:232301, 2006.
- [6] Xingbo Zhao and Ralf Rapp. Transverse Momentum Spectra of  $J/\psi$  in Heavy-Ion Collisions. *Phys. Lett. B*, 664:253–257, 2008.
- [7] Nora Brambilla, Miguel Angel Escobedo, Jacopo Ghiglieri, Joan Soto, and Antonio Vairo. Heavy Quarkonium in a weakly-coupled quark-gluon plasma below the melting temperature. *JHEP*, 09:038, 2010.
- [8] Taesoo Song, Kyong Chol Han, and Che Ming Ko. Charmonium production in relativistic heavy-ion collisions. *Phys. Rev. C*, 84:034907, 2011.
- [9] Xiaojian Du, Shuai Y. F. Liu, and Ralf Rapp. Extraction of the Heavy-Quark Potential from Bottomonium Observables in Heavy-Ion Collisions. *Phys. Lett. B*, 796:20–25, 2019.
- [10] Wei-Jun Deng, Hui Liu, Long-Cheng Gui, and Xian-Hui Zhong. Charmonium spectrum and their electromagnetic transitions with higher multipole contributions. *Phys. Rev. D*, 95(3):034026, 2017.
- [11] Xingyu Guo, Shuzhe Shi, Nu Xu, Zhe Xu, and Pengfei Zhuang. Magnetic Field Effect on Charmonium Production in High Energy Nuclear Collisions. *Phys. Lett. B*, 751:215–219, 2015.
- [12] Helmut Satz. Colour deconfinement and quarkonium binding. *J. Phys. G*, 32:R25, 2006.
- [13] Yun-peng Liu, Zhen Qu, Nu Xu, and Peng-fei Zhuang.  $J/\psi$  Transverse Momentum Distribution in High Energy Nuclear Collisions at RHIC. *Phys. Lett. B*, 678:72–76, 2009.
- [14] Shile Chen and Min He. Heavy quarkonium dissociation by thermal gluons at next-to-leading order in the Quark-Gluon Plasma. *Phys. Lett. B*, 786:260–267, 2018.
- [15] D. Blaschke, O. Kaczmarek, E. Laermann, and V. Yudichev. Heavy quark potential and quarkonia dissociation rates. *Eur. Phys. J. C*, 43:81–84, 2005.
- [16] Xingyu Guo, Shuzhe Shi, and Pengfei Zhuang. Relativistic Correction to Charmonium Dissociation Temperature. *Phys. Lett. B*, 718:143–146, 2012.
- [17] Shuzhe Shi, Xingyu Guo, and Pengfei Zhuang. Flavor Dependence of Meson Melting Temperature in Relativistic Potential Model. *Phys. Rev. D*, 88(1):014021, 2013.
- [18] Yan Wu, Defu Hou, and Hai-cang Ren. Relativistic correction of the quarkonium melting temperature with a holographic potential. *Phys. Rev. C*, 87(2):025203, 2013.

- [19] H. W. Crater and P. Van Alstine. Two-body Dirac Equations for Particles Interacting Through World Scalar and Vector Potentials. *Phys. Rev. D*, 36:3007–3036, 1987.
- [20] Peter Long and Horace W Crater. Two-body dirac equations for general covariant interactions and their coupled schrödinger-like forms. *J. Math. Phys.*, 39:124, 1998.
- [21] Bin Liu and Horace Crater. Two-body Dirac equations for nucleon-nucleon scattering. *Phys. Rev. C*, 67:024001, 2003.
- [22] Horace W. Crater and Cheuk-Yin Wong. Magnetic States at Short Distances. *Phys. Rev. D*, 85:116005, 2012.
- [23] Martin Schroedter, Robert L. Thews, and Johann Rafelski.  $B_c$  meson production in nuclear collisions at RHIC. *Phys. Rev. C*, 62:024905, 2000.
- [24] Faisal Akram and M. A. K. Lodhi.  $B_c$  absorption cross sections by nucleons. *Nucl. Phys. A*, 877:95–106, 2012.
- [25] Yunpeng Liu, Carsten Greiner, and Andriy Kostyuk.  $B_c$  meson enhancement and the momentum dependence in Pb + Pb collisions at energies available at the CERN Large Hadron Collider. *Phys. Rev. C*, 87(1):014910, 2013.
- [26] Wanda M. Alberico, Stefano Carignano, Piotr Czernski, Arturo De Pace, Marzia Nardi, and Claudia Ratti. Survival of  $B_c$  mesons in a hot plasma within a potential model. *Central Eur. J. Phys.*, 12(11):780–784, 2014.
- [27] Baoyi Chen, Liuyuan Wen, and Yunpeng Liu.  $B_c^+$  Formation from Random Charm and Anti-bottom Quarks in the Quark-Gluon Plasma. 11 2021.
- [28] Armen Tumasyan et al. Observation of the  $B_c^+$  Meson in Pb-Pb and pp Collisions at  $\sqrt{s_{NN}}=5.02$  TeV and Measurement of its Nuclear Modification Factor. *Phys. Rev. Lett.*, 128(25):252301, 2022.
- [29] Horace W. Crater, Jin-Hee Yoon, and Cheuk-Yin Wong. Singularity Structures in Coulomb-Type Potentials in Two Body Dirac Equations of Constraint Dynamics. *Phys. Rev. D*, 79:034011, 2009.
- [30] S. Digal, O. Kaczmarek, F. Karsch, and H. Satz. Heavy quark interactions in finite temperature QCD. *Eur. Phys. J. C*, 43:71–75, 2005.
- [31] R.L. Workman et al. The Review of Particle Physics. to be published in *Prog. Theor. Exp. Phys*, 2022.